Title: Seascape genomics as a new tool to empower coral reef conservation strategies: an example on north-western Pacific *Acropora digitifera*.

Running Title: Seascape genomics to support coral conservation

List of Authors: Oliver Selmoni[1], Estelle Rochat[1], Gael Lecellier[2,3], Veronique Berteaux-Lecellier[2], Stéphane Joost[1].

Institutional Affiliations:

[1] Laboratory of Geographic Information Systems (LASIG), School of Architecture, Civil and Environmental Engineering, Ecole Polytechnique Fédérale de Lausanne (EPFL), 1015 Lausanne, Switzerland

[2] UMR250/9220 ENTROPIE IRD-CNRS-UR, Labex CORAIL, Promenade Roger-Laroque, Noumea cedex, New Caledonia

[3] UVSQ, Université de Paris-Saclay, 45 avenue des Etats-Unis, Versailles Cedex, France

Contact Information:

Stéphane Joost: stephane.joost@epfl.ch, +41216935782

Abstract

Coral reefs are suffering a major decline due to the environmental constraints imposed by climate change. Over the last 20 years, three major coral bleaching events occurred in concomitance of anomalous heat waves, provoking a severe loss of coral cover worldwide. The conservation strategies for preserving reefs, as they are implemented now, cannot cope with global climatic shifts. Consequently, researchers are advocating the set-up of preservation frameworks to reinforce coral adaptive potential. However, the main obstacle to this implementation is that studies on coral adaption are usually hard to generalize at the scale of a reef system.

Here, we study the relationships between frequencies of genetic markers with that of environmental characteristics of the sea (seascape genomics), in combination with connectivity analysis, to investigate the adaptive potential of a flagship coral species of the Ryukyu Archipelago (Japan). By associating genotype frequencies with descriptors of historical environmental conditions, we discovered six genomic regions hosting polymorphisms that might promote resistance against thermal stress. Remarkably, annotations of genes in these regions were consistent with molecular roles associated with heat responses. Furthermore, we combined information on genetic and spatial distances between reefs to predict connectivity at a regional scale.

The combination between the results of these analyses portrayed the adaptive potential of this population: we were able to identify reefs carrying potential adaptive genotypes and to understand how they disperse to neighbouring reefs. This information was summarized by objective, quantifiable, and mappable indices covering the whole region, which can be extremely useful for future prioritization of reefs in conservation planning. This framework is transferable to any coral species on any reef system, and therefore represents a valuable tool for empowering preservation efforts dedicated to the protection of coral reef in warming oceans.

Keywords

Coral reefs – local adaptation – seascape genomics – conservation genomics – connectivity analysis

Acknowledgements

We thank Annie Guillaume and François Bonhomme for the useful comments and suggestions provided during the redaction of this paper.

Abstract

Coral reefs are suffering a major decline due to the environmental constraints imposed by climate change. Over the last 20 years, three major coral bleaching events occurred in concomitance of anomalous heat waves, provoking a severe loss of coral cover worldwide. The conservation strategies for preserving reefs, as they are implemented now, cannot cope with global climatic shifts. Consequently, researchers are advocating the set-up of preservation frameworks to reinforce coral adaptive potential. However, the main obstacle to this implementation is that studies on coral adaption are usually hard to generalize at the scale of a reef system.

Here, we study the relationships between frequencies of genetic markers with that of environmental characteristics of the sea (seascape genomics), in combination with connectivity analysis, to investigate the adaptive potential of a flagship coral species of the Ryukyu Archipelago (Japan). By associating genotype frequencies with descriptors of historical environmental conditions, we discovered six genomic regions hosting polymorphisms that might promote resistance against thermal stress. Remarkably, annotations of genes in these regions were consistent with molecular roles associated with heat responses. Furthermore, we combined information on genetic and spatial distances between reefs to predict connectivity at a regional scale.

The combination between the results of these analyses portrayed the adaptive potential of this population: we were able to identify reefs carrying potential adaptive genotypes and to understand how they disperse to neighbouring reefs. This information was summarized by objective, quantifiable, and mappable indices covering the whole region, which can be extremely useful for future prioritization of reefs in conservation planning. This framework is transferable to any coral species on any reef system, and therefore represents a valuable tool

for empowering preservation efforts dedicated to the protection of coral reef in warming oceans.

Keywords (6-10)

Coral reefs – Local adaptation – climate change – seascape genomics – coral bleaching – conservation genomics – Acropora digitifera – Ryukyu Archipelago

Introduction

Coral reefs are suffering a severe decline due to the effects of climate change (Hughes et al., 2017). Loss of reef is already showing catastrophic consequences for marine wildlife who depend on these structures (Pratchett et al., 2018), with disastrous aftermaths expected for human economies as well (Moberg & Folke, 1999). One of the major threats to the persistence of these ecosystems is coral bleaching (Bellwood et al., 2004): a physiological response induced by environmental stress that provokes hard-skeleton corals, the cornerstone of reefs, to separate from the symbiotic microbial algae essential for its survival (Mydlarz et al., 2010). Over the last 20 years, episodes ofcoral bleaching struck world-wide and resulted in a local coral cover loss of up to 50% (Hughes et al., 2017, 2018). Thermal stress is considered the main driver of coral bleaching (Hughes et al., 2017), but additional causes of anthropogenic origin were also identified (e.g. ocean acidification, water eutrophication, sedimentation and overfishing; Anthony et al., 2008; Ateweberhan et al., 2013; Maina et al., 2008).

Conservation efforts to mitigate the threat of coral bleaching tend to focus on restoring reefs that have undergone severe losses, as well as try to limit the impact of future bleaching events (Baums, 2008; Bellwood et al., 2004; Young et al., 2012). To achieve these aims, two main strategies are currently used: establish marine protected areas (MPAs) at reefs, and develop coral nurseries (Baums, 2008; Bellwood et al., 2004; Young et al., 2012). MPAs are designated zones in which human access and activities are severely restricted in order to alleviate the effects of local anthropogenic stressors (Lester et al., 2009). Coral nurseries are underwater gardens of transplanted colonies that can then be transplanted to restore damaged reefs (Baums, 2008; Young et al., 2012). For both conservation strategies, researchers advocate the use of methods that account for demographic connectivity such that the location of a conservation measure can also promote resistance and resilience for neighbouring sites (Baums, 2008; Krueck et al., 2017; Lukoschek et al., 2016; Palumbi, 2003; Shanks et al., 2003). Despite the

57 observed beneficial effects of these conservation policies worldwide (Cinner et al., 2016;
58 Rodgers et al., 2017; Selig & Bruno, 2010), these solutions do not confer resistance against the
59 temperature oscillations associated with the last mass bleaching events (Baums, 2008; Hughes
60 et al., 2017). Coral reefs that had experienced previous thermal stress were found to be more
61 resistant to subsequent heat waves (Hughes et al., 2019; Krueger et al., 2017; Penin et al., 2013;
62 Thompson & van Woesik, 2009), but to date this information is neglected in conservation
63 actions (Baums, 2008; Maina et al., 2011). There is an urgent need to understand whether these
64 observations are due to evolutionary processes and, if so, to determine how the underlying
65 adaptive potential could be included in predictions of climate change responses and in
66 conservation programs (Baums, 2008; Logan et al., 2014; Maina et al., 2011; van Oppen et al.,
67 2015a).
68 To this end, seascape genomics tools are likely to play an important role. Seascape genomics
69 is the marine counterpart of landscape genomics, a branch of population genomics that
70 investigates adaptive potential through field-based experiments (Balkenhol et al., 2017).
71 Samples that are collected across a landscape are genotyped using next-generation-sequencing
72 techniques, providing thousands of genetic variants, while simultaneously the environmental
73 variables of the study area are characterized, usually using remote-sensing data to describe
74 specific local climatic conditions (Leempoel et al., 2017). Genomics and environmental
75 information are then combined to detect genetic polymorphisms associated with particular
76 conditions (*i.e.,* potentially adaptive genotypes; Rellstab et al., 2015). This approach has been
77 applied to many terrestrial species, and is increasingly being used to analyse marine systems
78 in what is referred to as *seascape genomics* (exhaustively reviewed in Riginos, Crandall,
79 Liggins, Bongaerts, & Treml, 2016). To our knowledge no seascape genomics experiment has
80 yet been applied to reef corals. In fact, adaptation of these species has been mostly studied via
81 transplantation assays coupled with aquarium conditioning, which is a time- and resource-

82 demanding approach that is often restricted to a couple of reefs experiencing contrasting
83 conditions (Howells et al., 2013; Krueger et al., 2017; Palumbi et al., 2014; Sampayo et al.,
84 2016; Ziegler et al., 2017). Genotype-environment associations studies have also been
85 conducted on corals, but have used either a limited number of markers (<10 SNPs in Lundgren,
86 Vera, Peplow, Manel, & van Oppen, 2013), a restricted number of locations (two in Bay &
87 Palumbi, 2014), or focused on populations with restricted gene flow (L. Thomas et al., 2017).
88 Contrary to these previous studies, a seascape genomics approach should cover ecologically
89 meaningful spatial scales and be able to distinguish the pressures caused from different climatic
90 conditions, as well as account for confounding effects of demographic processes (Balkenhol
91 et al., 2017).
92 In the present study, we applied a seascape genomics framework to detect coral reefs that are
93 carrying potentially adaptive genotypes, and in turn, to show how conservation policies could
94 implement the results. Our study focuses on *Acropora digitifera* of the Ryukyu Archipelago in
95 Japan (Figure 1), an emblematic species of the Indo-Pacific and flagship organism for studies
96 on corals genomics (Shinzato et al., 2011). We first analysed the convergence between genomic
97 and environmental information to i) detect loci potentially conferring a selective advantage,
98 and ii) develop a model describing connectivity patterns. Next, we took advantage of these
99 findings to indicate which reefs were more likely to be carrying adaptive genotypes and to
100 evaluate their interconnectedness with the rest of the reef system. Finally, we propose an
101 approach to implement the results obtained into conservation planning. Overall, our work
102 provides tools for the interface between conservation genomics and marine environmental
103 sciences, which are likely to empower preservation strategies for coral reefs into the future.
104
105 **Materials and methods**

106 Our framework is structured on two axes of analysis and prediction: one focusing on the
107 presence of adaptive genotypes (seascape genomics), and the other on population connectivity
108 (Fig. 2). The seascape genomics analysis (Fig. 2A) combines genomic data with environmental
109 information to uncover potentially adaptive genotypes at sampling sites. The model describing
110 this relationship is then used to predict, at the scale of the whole study area, the probability of
111 the presence of adaptive genotypes (Fig. 2B). In the connectivity study (Fig. 2C), we made a
112 model describing how distances based on sea currents (calculated on the basis of remote
113 sensing data) correspond to the genetic separation between sites. This model is then used to
114 predict connectivity of sites at the study area scale (Fig. 2D). Finally, the predictions of where
115 the adaptive genotypes are more likely to exist, and of how the reef system is interconnected,
116 allow the assessment of adaptive potential across the whole study area (Fig. 2E).

117 *Genomic dataset*

118 The genomic data used come from a publicly available dataset consisting of 155 geo-referenced
119 colonies of *A. digitifera* from 12 sampling locations (13±5 colonies per site) of the Ryukyu
120 Archipelago in Japan (Fig. 1; Bioproject Accession PRJDB4188). These samples were
121 sequenced using a Whole-Genome Sequencing approach in the scope of a population genomics
122 study. Details on how samples were collected and processed for genomic analysis can be found
123 in Shinzato et al. (2015).

124 Genomic data were processed using the Genome Analysis Toolkit framework (GATK;
125 McKenna et al., 2010) following the recommended pipeline (the "GATK Best Practices"; Van
126 der Auwera et al., 2013) with the necessary modifications for coping with the absence of
127 reliable databases of known variants for this species. In short, the *A. digitifera* reference
128 genome (v. 1.1, GenBank accession: GCA_000222465.2; Shinzato et al., 2011) was indexed
129 using bwa (v. 0.7.5a, Li & Durbin, 2009), samtools (v. 1.9, Heng Li et al., 2009) and
130 picard-tools (v. 1.95, http://broadinstitute.github.io/picard) and raw sequencing reads were

131 aligned using the bwa *mem* algorithm. The resulting alignments were sorted, marked for
132 duplicate reads, modified for read-group headers and indexed using picard-tools. Next, each
133 alignment underwent an independent variant discovery using the GATK HaplotypeCaller tool
134 (using the ERC mode and setting the --minPruning flag to 10) and genotypes were then jointly
135 called by the GATK GenotypeGVCFs tool in random batches of 18 samples to match our
136 computational power (18 CPUs). The variant-calling matrices of the different batches were
137 then joined and filtered in order to keep only bi-allelic Single Nucleotide Polymorphisms
138 (SNPs) using the GATK CombineVariants and SelectVariants tools, respectively. This resulted
139 in a raw genotype matrix counting ~1.2 M of SNPs. Subsequently, we used the GATK
140 VariantAnnotator tool to annotate variants for Quality-by-depth and filtered for this value (<2),
141 read coverage (>5 and <100 within a sample), minor allele frequency (>0.05), major genotype
142 frequency (<0.95) and missing rate of both individuals and SNPs (<0.1) using the GATK
143 VariantFiltrationTool and custom scripts in the R environment (v. 3.5.1, R Core Team, 2016).
144 Finally, we filtered for linkage disequilibrium using the *snpgdsLDpruning* function of the
145 SNPrelate R package (v. 1.16, LD threshold=0.3; Zheng et al., 2012). This pipeline produced
146 the filtered genotype matrix consisting of 136 individuals and 7,607 SNPs.
147 Natural hybridization and transient species boundaries have been observed in *Acropora* species
148 (Van Oppen et al., 2002). We investigated these hypotheses by running a preliminary analysis
149 of fixation index (Fst) variation by genomic position using the R KRIS package (v. 1.1;
150 Chaichoompu et al., 2018). Since we found no genomic islands of low-recombination (i.e. high
151 Fst; Nosil et al., 2009) between the populations of Kerama, Yaeayama and Okinawa (Fig. S1)
152 we excluded the possibility of presence of genetically isolated groups in the dataset.
153 Importantly, previous studies on this coral population did not report hybridization with other
154 species, neither the presence of cryptic species nor isolated sub-populations (Nakajima et al.,
155 2010; Nishikawa, 2008; Shinzato et al., 2015).

156

157 *Environmental data*

158 Twelve georeferenced datasets describing atmospheric and seawater conditions were retrieved
159 from publicly available resources (EU Copernicus Marine Service, 2017; NASA, 2016;
160 National Oceanic and Atmospheric Administration, 2017; Table S1). These remote sensing
161 derived datasets provide monthly or daily variables measured over several (on average 14)
162 years before the genetic data were sampled (2010; Shinzato et al., 2015). The data cover the
163 entire study area (Fig. 1), with a spatial resolution ranging from 25 km to 4 km (Tab. S1). We
164 processed these variables in the R environment using the *raster* package (v. 2.8, Hijmans, 2016)
165 to compute monthly averages and standard deviations for the entire study period. Furthermore,
166 Sea Surface Temperature (SST) measurements were used to compute a Degree Heat Week
167 (DHW) frequency index, representing the percentage of days during which the bi-weekly
168 accumulated heat stress exceeded 4 °C (Liu et al., 2003; Logan et al., 2014). SST and sea
169 surface salinity records were combined to produce estimates of seawater pH (Covington &
170 Whitfield, 1988), dissolved inorganic carbon (Loukos et al., 2000), and alkalinity (Lee et al.,
171 2006). Bathymetry data (Ryan et al., 2009) were used to retrieve the depth at sampling
172 locations. Finally, population density data (CIESIN Columbia University, 2010) were averaged
173 in a 50 km buffer area to produce a surrogate-variable for anthropogenic pressure (Welle et al.,
174 2017).

175 We used the geographic coordinates associated with each sample to characterize the
176 environmental conditions using the QGIS point sampling tool (v. 2.18.25, QGIS development
177 team, 2009). For the predictive step of our study (Fig. 2C) at the scale of the whole reef system
178 we retrieved the shapes of the reefs of the region (UNEP-WCMC et al., 2010) and reported
179 them into a regular grid (cell size of 5x5 km) using QGIS. For the reef cells smaller than a 5-
180 by-5 km square, we calculated the actual area (in km^2). Reefs from the neighbouring regions

181 (Taiwan and Philippines, Fig. 1) were also included to avoid border-effects in computations.
182 Environmental conditions were assigned to each reef-cell using the average function of the
183 QGIS zonal statistics tool.
184
185 *Seascape genomics*
186 We performed the genotype-environment association analysis using the logistic regression
187 method implemented within the SamBada software (v. 0.7; Stucki et al., 2017), customized to
188 speed-up multivariate models computation in the Python environment (v. 2.7; Python Software
189 Foundation, 2018) using the *pandas* (v. 0.23.4; McKinney, 2010) and *statsmodels* (v. 0.9;
190 Seabold & Perktold, 2010) libraries. The SamBada approach allows proxy variables of genetic
191 structure to be included in the analysis in order to avoid possible confounding effects (patterns
192 of neutral genetic variation mimicking signals of adaptation to the local environment;
193 Holderegger et al., 2008). Here we performed a discriminant analysis of principal components
194 (DAPC) on the SNPs genotype matrix using the R package *adegenet* (v. 2.1.1; Jombart, 2008).
195 This procedure highlighted a main separation between two groups of samples along the first
196 discriminant function (Fig. S2). The latter was therefore used as co-variable in association
197 models. We then ran the pipeline for the discovery of adaptive signals described below and
198 summarized in a schematic in Fig. S3. In order to speed up calculations, the 315 environmental
199 variables were grouped into 29 clusters of highly correlated (Pearson method, $|R|>0.7$)
200 descriptors in the R environment (Fig. S3A). For each of these groups, one variable was
201 randomly selected to build logistic models against the three genotypes of each SNP (Fig. S3B).
202 In total, the SamBada instance evaluated 661,809 association models (29 environmental groups
203 against 3 x 7,607 SNPs; Fig. S3C, S2D) that were subsequently analysed in the R environment.
204 For each association-model related to the same environmental variable, p-values of G-scores
205 (G) and Wald-scores (W) were corrected for multiple testing using the R *q-value* package (v.

206 2.14, Storey, 2003). Association models scoring q<0.001 for both statistics were deemed
207 significant (Fig. S3E). If a SNP was found in more than one significant association, only the
208 best model (according to the value of G) was kept. For each significant association retained,
209 we then calculated all the models built with the focal SNP against the other environmental
210 variables from the same correlated descriptor cluster, and we looked for the best association
211 model (according to G; Fig. S3F). The best association model for each significant SNP is
212 hereafter referred to as the significant genotype-environment association (SGEA). Finally, we
213 visualized the logistic regression of each significant SGEA using the R *popbio* library (v. 2.4.4;
214 Stubben & Milligan, 2007).
215
216 *Annotation of seascape genomics results*
217 We then annotated the genomic neighbourhood of each SGEA in order to discover genes
218 potentially linked to an adaptive role. We set the size of the search window to ±250 kbs around
219 the concerned SNP of each SGEA. This window size was selected because genes(s) possibly
220 linked to a mutation may lay up to hundreds of kbs away (Brodie et al., 2016; Visel et al.,
221 2009), and this window size corresponds approximately to the scaffold N50 statistics of the
222 reference genome (*i.e.* half of the genome is contained within scaffolds of this size or longer).
223 For every SGEA, the annotation procedure was performed as follows. Based on the NCBI
224 annotation of the reference genome
225 (https://www.ncbi.nlm.nih.gov/genome/annotation_euk/Acropora_digitifera/100/), we
226 retrieved all the predicted genes falling within the ±250 kbs window. Next, we retrieved the
227 predicted protein sequences related to these genes and ran a similarity search (blastp, (Madden
228 & Coulouris, 2008) against metazoan protein sequences in the swissprot database (release
229 2019_07; Boeckmann et al., 2003). For every predicted gene, only the best significant match
230 (E-score threshold < 10^{-7}) was kept. Finally, predicted genes were annotated with the

231 eukaryotic cluster of orthologous genes (KOG; Jensen et al., 2008) annotation from the
232 matching swissprot entry. For every KOG we calculated the relative frequency across the *A.*
233 *digitifera* genome. This was obtained by dividing the genome into 500 kbs windows and by
234 calculating the percentage of windows in which the KOG was observed.
235
236 *Probability of Presence of Adaptive Genotypes*
237 The results of the seascape genomics analysis were then used to predict the probability of the
238 presence of adaptive genotypes at the scale of the whole Ryukyu Archipelago (Fig. 2B). For
239 each SGEA, the SamBada approach provides parameters of a logistic regression that links the
240 probability of occurrence of the genotype with the value of the environmental variable (Stucki
241 et al., 2017). These logistic models can therefore be used to estimate the probability of presence
242 of the genetic variant for any value of the environmental variable (Joost, 2006; Rochat, E.,
243 Leempoel, K., Vajana, E., Colli, L., Ajmone-Marsan, P., Joost, 2016). We assumed that
244 potentially adaptive genotypes could reach any reef of the region since several studies reported
245 migration events between distant islands of the Archipelago (Nakajima et al., 2010; Nishikawa,
246 2008; Shinzato et al., 2015). Finally, these probabilities where combined into an average
247 probability (i.e. the arithmetical mean) of carrying adaptive genotypes (P_a) at each reef of the
248 Ryukyu Archipelago.
249
250 *Sea current data*
251 Daily records of sea surface current were retrieved from publicly available databases (zonal
252 and meridional surface velocities from the *global-reanalysis-phy-001-030* product; EU
253 Copernicus Marine Service, 2017) and used to compute the direction and speed of currents in
254 the R environment using the *raster* library. By using the resample function of the R *raster*
255 library, we increased resolution of these data from original 0.083° (~9.2 km) to 0.015° (~1.6

256 km) and corrected land pixels (*i.e.* removing sea current values) using an high-resolution
257 bathymetry map (Ryan et al., 2009). These day-by-day records of sea currents (from 1993 to
258 2010) were then stacked to retrieve, for each pixel of the study area, the cumulated speed
259 toward each of the eight neighbouring pixels. For every pixel, the cumulated speed in each of
260 the eight directions was divided by the total speed (the sum of the eight directions) to obtain
261 the probability of transition in each direction (the conductance). This information was used to
262 calculate dispersal costs (the inverse of the square conductance) and was summarized in a
263 transition matrix in the format of the R *gdistance* package (v. 1.2, van Etten, 2018). For the
264 connectivity analysis (Fig. 2C), the transition matrix was used to calculate sea distances (*i.e.*
265 the least-cost path) between sampling sites of the genotyped colonies. For the connectivity
266 predictions (Fig. 2D), we calculated the sea distances between all the reefs of the study area,
267 whose coordinates were the centroids of the reef-cells computed as described in the
268 environmental variables section. Importantly, for each pair of reefs (for instance $reef_1$ and $reef_2$)
269 two sea distances were computed, one for each direction (*i.e.* from $reef_1$ to $reef_2$ and from $reef_2$
270 to $reef_1$).
271
272 *Connectivity analysis*
273 Genetic distances between sampling sites were calculated using the pairwise F-statistics (Fst;
274 Weir & Cockerham, 1984) as implemented in the R *hierfstat* library (v. 0.04; Goudet, 2005).
275 When there is no dispersal constraint between two sub-populations, the related Fst is equal
276 to zero. Conversely, when dispersal is constrained, Fst increases up to a maximum value of one
277 (isolated sub-populations). To avoid bias due to low sample sizes, we only considered sample
278 sites with more than 10 samples each (7 out of 12).
279 Next, we built a linear model (hereafter referred to as the connectivity model) to estimate Fst
280 from the sea distances between each pair of sample sites. Since each pair of sites was connected

281 by two distances (from $reef_1$ to $reef_2$ and *vice versa*), we built three models based on shortest,
282 longest and average sea distance between each pair. As an additional comparison, we also built
283 a connectivity model using Euclidean distances of coordinates as independent variable while
284 maintaining Fst as response variable. For each model, we then ran a t-test to check for the
285 statistical significance of the relationship between genetic and geographical distance. Next, we
286 compared the four models by relying on the coefficients of determination (R2) and the Akaike
287 information criterion (AIC; Bozdogan, 1987) to identify the best connectivity model to use in
288 connectivity predictions.
289
290 *Connectivity Predictions*
291 The best connectivity model defined in the connectivity analysis was used to calculate the
292 predicted Fst (pFst) between all pairs of reefs of the Ryukyu Archipelago. To this end, we
293 translated sea distances in pFst using the connectivity model trained during the connectivity
294 analysis. Importantly, since there are two sea distances connecting each pair of reefs, two pFst
295 were computed as well (Fig. S5). Based on these predictions, we were able to calculate two
296 indices for each reef-cell:
297 - *outbound connectivity index* (OCI; Fig. 4a): the sum of the area (in km^2) of all the reefs
298 connected under a specific pFst threshold <u>from</u> the focal reef.
299 - *inbound connectivity index* (ICI; Fig. 4b): the sum of the area (in km^2) of all the reefs
300 connected under a specific pFst threshold <u>to</u> the focal reef.
301 These connectivity indices and their interpretation are subordinate to the pFst threshold
302 applied in the calculation. For this reason, it is crucial to set this threshold by considering the
303 size of the study area and the distribution of the pFst values observed (Fig. S5). In this work,
304 we set the pFst threshold to 0.02. In fact, a smaller pFst (for ex. 0.01; Fig. S5) would have
305 informed on local connectivity only (within neighbouring islands) and neglect connectivity at

306 the scale of the Ryukyu Archipelago. In contrast, a higher pFst (for ex. 0.05, Fig. S5) would
307 have exceeded the study area boundaries, causing bias (border effects) in the calculation of the
308 indices for reefs of the southern Islands (Yaeyama and Miyako) of the Archipelago.
309
310 *Evaluation of the adaptive potential*
311 The adaptive potential was evaluated by combining the predictions of the presence of adaptive
312 genotypes (P_a) and connectivity patterns (ICI) in an *index of adaptive potential* (API, Fig. 2E).
313 Indeed, API is a special case of ICI calculated as the sum of the weighted area (in km^2) of all
314 the reefs connected under a specific pFst threshold to the focal reef. The weight applied to each
315 reef corresponded to the probability of carrying adaptive gentoypes (P_a). For the pFst threshold,
316 we used the same value (0.02) as employed in the ICI and OCI calculations.
317
318 **Results**
319 *Seascape Genomics*
320 We detected 6 significant genotype-environment associations (SGEA, q_G and
321 q_W<0.001, Tab.1) spanning across 6 distinct scaffolds of the *A. digitifera* reference genome.
322 Among them, one SGEA was related to SST variation in April and the others to degree heat
323 week (DHW) frequency.
324 SGEA1 described the relationship between SST standard deviation in April and one SNP
325 located within a genomic window (± 250 kb) counting 18 predicted genes, 3 of which annotated
326 to the eukaryotic cluster of orthologs (KOGs) *Signal sequence receptor delta*, *DNA helicase*,
327 *transposon protein* (Tab. 1, Box S1). All the remaining SGEAs (SGEA2-6) were related to
328 DHW frequency only. In SGEA2, the concerned SNP was surrounded by 21 predicted genes,
329 6 of which annotated with KOGs *splicing factor U2AF*, *G- protein-coupled receptor*,
330 *geranylgeranyl diphosphate synthase*, *Cytochrome p450*, *receptor*, *NFU1 iron-sulfur cluster*

331 *scaffold homolog* (Tab.1, Box S2). In SGEA3, the SNP was surrounded by 14 predicted genes,
332 with 3 KOGs annotated as *protein kinase, leucine rich repeat* and *jnk1 mapk8-associated*
333 *membrane protein* (Tab. 1, Box S3). In SGEA4, 5 and 6, the SNPs were located in genomic
334 windows counting 11, 5 and 1 predicted genes, respectively, and each containing the same two
335 KOGs: *DNA helicase* and *Exonuclease 3'-5' domain containing 2* (Tab. 1*;* Box S4, S5, S6).
336
337 *Probability of Presence of Adaptive Genotypes*
338 The SGEAs of the seascape genomics analysis were then used as the starting point for
339 predicting the probability of presence of adaptive genotypes (P_a) across the reefs of the region.
340 Since most of the putative adaptive genotypes were found to be associated with DHW
341 frequency (SGEA2-6; Tab. 1), we chose this variable as the environmental pressure of interest.
342 The average of P_a ranged from 0 to 1 (Fig. 3). In Ryukyu Archipelago, P_a was higher in Miyako
343 ($\overline{P_a}_{Miyako} = 0.55 \pm 0.22$) and Okinawa ($\overline{P_a}_{Okinawa} = 0.4 \pm 0.24$), lower in Amami
344 ($\overline{P_a}_{Amami} = 0.22 \pm 0.15$) and Yaeyama ($\overline{P_a}_{Yaeyama} = 0.22 \pm 0.12$), and close to zero in the
345 north of the region (Tokara and Osumi; $\overline{P_a}_{Tokara} = 0.02 \pm 0.04$, $\overline{P_a}_{Osumi} = \sim 0$; Fig. 3).
346 Outside the Ryukyu Archipelago, a high P_a (>0.7) was predicted in northern Philippines while
347 reefs around Taiwan displayed in general low P_a (<0.4; Fig. 3).
348
349 *Connectivity modelling*
350 The connectivity model based on the shortest sea distances between pairs of sites was the best
351 to describe Fst variation (R2=0.72, AIC=-234; Fig. S4a), compared to models based on the
352 longest sea distance (R2=0.62, AIC=-227, Fig. S4b), the average sea distance (R2=0.66, AIC=-
353 230, Fig. S4c), and the aerial distance (R2=0.66, AIC=-230, Fig S3d). The connectivity indices
354 were therefore computed using the connectivity model based on the shortest sea distance
355 between sites.

The ICI variation followed a north to south decrease (Fig. 4a). The reefs around the islands in the north of the archipelago (Osumi, Tokara and Amami) were generally those with the highest ICI ($\overline{ICI}_{Tokara} = 1615 \pm 229\ km^2$; $\overline{ICI}_{Amami} = 1209 \pm 28\ km^2$; $\overline{ICI}_{Osumi} = 1164 \pm 336\ km^2$; Fig. 4a). In the central area (Okinawa), ICI was lower ($\overline{ICI}_{Okinawa} = 999 \pm 42\ km^2$), while the lowest ICI values were observed in the southern area (Yaeyama and Miyako; $\overline{ICI}_{Miyako} = 777 \pm 71\ km^2$; $\overline{ICI}_{Yaeyama} = 674 \pm 76\ km^2$; Fig. 4a).

With regards to OCI, we observed a decrease in index with latitude (Fig. 4b). OCI was highest in the southern half of the archipelago (Yaeyama, Miyako and Okinawa; $\overline{OCI}_{Yaeyama} = 1014 \pm 2\ km^2$; $\overline{OCI}_{Miyako} = 1008 \pm 14\ km^2$; $\overline{OCI}_{Okinawa} = 936 \pm 91 km^2$; Fig. 4b). A lower OCI was observed in the northern part (Amami and Tokara; $\overline{OCI}_{Amami} = 766 \pm 51\ km^2$; $\overline{OCI}_{Tokara} = 706 \pm 2\ km^2$; Fig. 4b), while the extreme north of the Archipelago (Osumi) had a very low OCI ($\overline{OCI}_{Osumi} = 6 \pm 4\ km^2$; Fig. 4b).

Evaluation of the adaptive potential

The variations of API were generally structured along the latitudinal axis (Fig. 5). Reefs in the northern part of the Archipelago (Tokara, Amami and Osumi) generally showed the highest API values ($\overline{API}_{Tokara} = 391 \pm 7\ km^2$; $\overline{API}_{Amami} = 371 \pm 10\ km^2$; $\overline{API}_{Osumi} = 345 \pm 101\ km^2$; Fig. 5). In the central part of the study area (Okinawa), API was lower ($\overline{API}_{Okinawa} = 332 \pm 14\ km^2$; Fig. 5) and in the southern part the lowest API values were observed, ($\overline{API}_{Yaeyama}\ 233 \pm 20\ km^2$; $\overline{API}_{Miyako} = 280 \pm 28\ km^2$; Fig. 5).

Discussion

Adaptation to thermal stress

380 Thermal stress is expected to be one of the major threats to coral reef survival, where the
381 research for adaptive traits is becoming of paramount importance (Baums, 2008; Logan et al.,
382 2014; Maina et al., 2011). In the present study, the seascape genomics analysis of *A. digitifera*
383 of the Ryukyu Archipelago revealed the presence of 6 genomic regions hosting genetic variants
384 that might confer a selective advantage against thermal stress (Tab. 1). None of the SNPs
385 related to the SGEA lay directly within a coding sequence of a putative gene, but this is rarely
386 the case for causative-mutations (Brodie et al., 2016). In fact, genetic variants in intergenic
387 regions that play a modulatory action on the expression of neighbouring genes are more
388 frequent and can influence loci at a distance of 1-2 Mb (Visel et al., 2009). The fragmentation
389 of the reference genome forced us to limit our search window to ±250 Kb around each SNP,
390 yet we still found annotations corroborating a response to heat stress.
391 The SNP in SGEA3 was found to be related to KOG3744 (*jnk1 mapk8-associated membrane*
392 *protein;* Tab. 1). This KOG is rare across the genome of *A. digitifera* (with an expected
393 frequency of 0.0009 per 500 kbs window) and previous research corroborates the hypothesis
394 that this gene plays a role in thermal adaptation. Mitogen-activated-protein kinases (MAPKs)
395 are proteins known to be involved in cellular responses to stress across a range of taxa
396 (Neupane et al., 2013), and the c-Jun-N-terminal kinase (JNK) has previously been shown to
397 be activated under thermal stress in the coral *Stylopohora pistillata* (Courtial et al., 2017).
398 In SGEA1, 4, 5 and 6, one KOG recurred in the annotations: KOG0351 (*DNA helicase*; Tab.
399 1). The expected frequency of this KOG is 0.04 per 500 kbs window and remarkably we found
400 4 of them in 6 distinct 500 kbs windows around SGEA associated with thermal stress. These
401 orthologs annotate a particular type of DNA helicases (swissprot IDs: Q91920, Q14191)
402 known as “helicases Q” or “RecQ” (Box S1, 5-7), which are involved in the DNA repairing
403 mechanism caused by UV-light damage in prokaryotes (Courcelle & Hanawalt, 1999), and for
404 which light-stress driven effects were observed in eukaryotic cells as well (Sharma et al., 2006).

405 The modulation of this mechanism might therefore play a role in increasing *A. digitifera*
406 resistance against light-stress associated with heat waves.
407 Seascape/Landscape genomics studies are susceptible to high false discovery rates, especially
408 when neutral genetic structure is not accounted for (Rellstab et al., 2015). To take this element
409 into account, we processed data following a conservative pipeline and used models explicitly
410 integrating demographic processes. We also set a restrictive threshold to filter significant
411 association-models (*i.e.* q<0.001 in two distinct tests). Most of the SGEA found were linked to
412 DHW, most probably because this variable represents one of the main constraints to coral
413 survival (Hughes et al., 2003). It is also possible that the initial application of a sampling
414 scheme adapted to seascape genomics (unlike the one used by Shinzato et al. 2015 who did not
415 consider environmental variability) would have increased sensitivity to other types of adaptive
416 signals (Riginos et al., 2016; Selmoni et al., 2019).
417 We found SGEA related to thermal stress displaying annotations corroborating a role in cellular
418 heat responses. Nonetheless, annotations analysis is only a first step in the validation of the
419 SGEA detected. Ideally, further assays as reciprocal transplantations (Palumbi et al., 2014),
420 experimental conditioning (Krueger et al., 2017) and molecular analysis (Courtial et al., 2017)
421 could ascertain and help quantifying the link between each genotype and the putative selective
422 advantage it might confer.
423
424 *Connectivity patterns*
425 Coral dispersal is driven by the water flow (Paris-Limouzy, 2011), which is highly
426 asymmetrical in this region (north-east oriented) due to the Kuroshio current (Nishikawa,
427 2008). As previously observed, the main patterns of migrations in this population occurs from
428 the south-west to the north-east (Shinzato et al., 2015). Reefs in the southern part of the study
429 area (Yaeyama and Miyako) showed the lowest ICI values (Fig. 4a), suggesting a potential

430 lack of recruits arriving from other reefs of the region. In fact, the genetic diversity of southern
431 reefs of the Ryukyu Archipelago is likely to depend on the recruits arriving from the east-coast
432 of Taiwan and the northern Philippines, which are located upstream of the Kuroshio current
433 (Fig. S5a; Chen & Shashank, 2009).
434 In the previous study on this data (Shinzato et al., 2015), reefs from Yaeyama resulted as those
435 with the lowest heterozygosity rates across the study area. This observation was attributed to a
436 population bottleneck caused by the 1998 bleaching event, but it is worth noting that reefs on
437 the west coast of Okinawa showed higher heterozygosity rates despite having suffered
438 recurrent bleaching events since 1998 (Donner et al., 2017). The lower heterozygosity rates in
439 Yaeyama therefore might reflect not only the effects of past bleaching, but also the relative
440 isolation of these islands from the reefs of the region (Fig. 4a).
441 In line with the same previous observations (Shinzato et al., 2015), the OCI value showed (Fig.
442 4b) that the southern reefs (Yaeyama and Miyako) are those expected to be the most prominent
443 source of recruits for the rest of the Archipelago. Given this crucial aspect, it is even more
444 important to preserve southern reefs of the Ryukyu Archipelago from the risks of isolation (e.g.
445 inbreeding depression; Keller & Waller, 2002).
446
447 *Adaptive potential in the 2016 bleaching event*
448 Reefs from islands of Miyako, Okinawa and the northern part of Amami were those most likely
449 to carry adaptive genotypes against thermal stress (Fig. 3). Previous work reported severe
450 bleaching in Okinawa in 1998 (Yamazato, 1999) and that adapted colonies might have resisted
451 (Van Woesik et al., 2004). In contrast, reefs in the northern part of the Archipelago (Amami,
452 Tokara and Osumi) experienced bleaching with moderate severity during the 1998 event
453 (Donner et al., 2017), which might explain why adaptive genotypes are not expected at the
454 same frequency (Fig. 3).

455 The adaptive potential index (API) defines the convergence between the probability of carrying
456 adaptive genotypes with connectivity predictions (Fig. 5). Reefs in the northern part of the
457 Archipelago (Amami, Tokara and Osumi) showed a higher API compared to those in the
458 southern half of the region (Okinawa, Yaeyama and Miyako). Two reasons may explain this
459 result: 1) these northern reefs are located downstream (on the Kuroshio Current) of two areas
460 where putative adapted reefs are frequent (Okinawa and Miyako; Fig. 3); 2) the region of
461 Northern Philippines, hosting high density of putative adapted reefs (Fig. 3), is more connected
462 to the northern part of the Ryukyu Archipelago than with the southern part (Fig. S6). This may
463 also explain why, despite hosting putative adapted reefs (Fig, 3), the Miyako area showed
464 among the lowest API values of the Archipelago (Fig. 5).
465 In 2016, the first mass bleaching event occurred in Japan since the Shinzato and colleagues
466 published the genetic data re-analysed in this work (Kimura et al., 2018). Field surveys related
467 to this bleaching event reported severe bleaching in Yaeyama (intensity up to 99%, mortality
468 up to 68%) and in Miyako (intensity up to 70%, mortality up to 67%; Tab. 2). In Okinawa and
469 Amami, the impact of this same bleaching event was moderate to mild (Okinawa: intensity up
470 to 48%, mortality up to 13%; Amami: intensity 8% and mortality 2%; Tab. 2). Reefs predicted
471 to show low API (the southern reefs) appeared to suffer more severe bleaching than those in
472 the northern region (which showed higher API; Fig. 5), but care must be taken in the
473 interpretation due to the confounding role of the degree of heat stress (Tab. 2).
474 Indeed, satellite records of sea temperature (EU Copernicus Marine Service, 2017) show that
475 in 2016 the number of days in temperature anomaly (DHW>4°C; Liu et al., 2003) was higher
476 in the southern part of the Archipelago (Yaeyama: ~81 days; Miyako: ~84 days) than in the
477 northern region (Okinawa: ~76 days; Amami: ~68; Tab. 2). Nevertheless, when two distant
478 sites had a comparable degree of heat stress, higher API was generally associated with a
479 reduced severity in bleaching. For instance, reefs in Kerama (Okinawa) and Sekisei Lagoon

North (Yaeyama) both suffered 81 days of heat stress in 2016, but the bleaching intensity in the Sekisei Lagoon was more than ten times higher than observed for Kerama (91% vs 7%), with a lower API (225 km^2 vs 334 km^2; Tab 2).

While these field observations seem to corroborate our predictions on adaptive potential, it is important to consider that they do not refer specifically to *A. digitifera,* but to the coral community as a whole (Kimura et al., 2018). Additionally, other local stressors (for instance anthropogenic pollution) might have modulated the bleaching response (Ateweberhan et al., 2013). Future bleaching surveys, with larger sample sizes and bleaching data referring to the specific coral genus, might provide a more reliable ground for validating our predictions.

Application in conservation

Conservation policies require objective and quantifiable information to prioritize areas for intervention efforts (OECD, 2017). In this study, we presented an original framework to calculate indices matching these requirements to describe the connectivity and adaptive potential against thermal stress of a flagship coral species of the north-western Pacific. Insights of this kind are essential for effective planning of coral conservation strategies (Baums, 2008; Logan et al., 2014; Palumbi, 2003; van Oppen et al., 2015b).

As they are derived from a universal metric of population connectivity (Fst; Weir & Cockerham, 1984), the indices we propose here are computable for any coral species. Thus, connectivity indices for different species can be compared or aggregated for conservation management planning within a region. Furthermore, each of the indices we propose is expressed in a tangible spatial unit (km^2) that allows for comparison between different datasets and areas.

As an example, the predictions from the connectivity indices can be used to support the planning of marine protected areas (MPAs; Box 1a). An ideal placement of an MPA should

505 ensure that the connectivity to the rest of the reef system is optimal (Krueck et al., 2017; C. J.
506 Thomas et al., 2014), and the OCI provides this information (Fig. 4b). Furthermore, the
507 computation of the ICI (Fig. 4a) from a protected area to the rest of the reef system could be
508 used to compare how different locations of MPAs may modify the connectivity to other specific
509 regions (Box 1a).
510 The indices proposed in this work could also support coral nursery establishment plans (Box
511 1b). In this type of conservation strategy, the transplantation of adapted colonies (*i.e.* those
512 carrying the adaptive genotypes) can be used to reinforce the adaptive potential of a population
513 (Baums, 2008; van Oppen et al., 2015b). Conservation managers can simulate the transplanting
514 procedure by setting P_a=1 at reefs where the nurseries will be established and then measure
515 how these changes would impact the API of the population (Box. 1b).
516 To date, the calculation of these indices can be performed using the R scripts and codes (R
517 Core Team, 2016) made publicly available in this research. In the future, however, this
518 framework should be transposed to a more user-friendly interface to facilitate its use by
519 conservation managers.
520
521 *Conclusions*
522 This study highlights the value of a seascape genomics approach for supporting the
523 conservation of corals. We applied it to a flagship coral species of the Ryukyu Archipelago and
524 identified genetic variants that may underpin adaptation to thermal stress. Coupling this
525 information with a genetic analysis of connectivity made it possible to evaluate the adaptive
526 potential at the scale of the entire study area. The outputs of this analysis are quantitative
527 indices that are could be used to support objective prioritization of reefs in conservation plans.
528 This framework is transferable to any coral species on any seascape and therefore constitutes
529 a useful conservation tool to evaluate the genomic adaptive potential of coral reefs worldwide.

Data Archiving Statement

All the data and codes used in this article will be made publicly available on Dryad after manuscript is accepted for publication.

Literature cited

Anthony, K. R. N., Kline, D. I., Diaz-Pulido, G., Dove, S., & Hoegh-Guldberg, O. (2008). Ocean acidification causes bleaching and productivity loss in coral reef builders. *Proceedings of the National Academy of Sciences of the United States of America*, *105*(45), 17442–6.

Ateweberhan, M., Feary, D. A., Keshavmurthy, S., Chen, A., Schleyer, M. H., & Sheppard, C. R. C. (2013). Climate change impacts on coral reefs: Synergies with local effects, possibilities for acclimation, and management implications. *Marine Pollution Bulletin*, *74*(2), 526–539.

Balkenhol, N., Dudaniec, R. Y., Krutovsky, K. V., Johnson, J. S., Cairns, D. M., Segelbacher, G., … Joost, S. (2017). Landscape Genomics: Understanding Relationships Between Environmental Heterogeneity and Genomic Characteristics of Populations (pp. 1–62). Springer, Cham.

Baums, I. B. (2008). A restoration genetics guide for coral reef conservation. *Molecular Ecology*, *17*(12), 2796–2811.

Bay, R. A., & Palumbi, S. R. (2014). Multilocus Adaptation Associated with Heat Resistance in Reef-Building Corals. *Current Biology*, *24*(24), 2952–2956.

Bellwood, D. R., Hughes, T. P., Folke, C., & Nyström, M. (2004, June 24). Confronting the coral reef crisis. *Nature*.

Boeckmann, B., Bairoch, A., Apweiler, R., Blatter, M. C., Estreicher, A., Gasteiger, E., … Schneider, M. (2003). The SWISS-PROT protein knowledgebase and its supplement TrEMBL in 2003. *Nucleic Acids Research*, *31*(1), 365–370.

Bozdogan, H. (1987). Model selection and Akaike's Information Criterion (AIC): The general theory and its analytical extensions. *Psychometrika*, *52*(3), 345–370.

Brodie, A., Azaria, J. R., & Ofran, Y. (2016). How far from the SNP may the causative genes be? *Nucleic Acids Research*, *44*(13), 6046–54.

Chaichoompu, K., Abegaz, F., Tongsima, S., James Shaw, P., Sakuntabhai, A., Pereira, L., & Van Steen, K. (2018). KRIS: Keen and Reliable Interface Subroutines for Bioinformatic Analysis version 1.1.1 from CRAN. Retrieved from https://cran.r-project.org/package=KRIS

Chen, C. A., & Shashank, K. (2009). Taiwan as a connective stepping-stone in the Kuroshio Triangle and the conservation of coral ecosystems under the impacts of climate change. *Kuroshio Science*, *3*(1), 15–22. Retrieved from https://ci.nii.ac.jp/naid/120001597275

CIESIN Columbia University. (2010). Gridded Population of the World (GPW), v3. Retrieved January 18, 2019, from http://sedac.ciesin.columbia.edu/data/set/gpw-v3-population-count

Cinner, J. E., Huchery, C., MacNeil, M. A., Graham, N. A. J., McClanahan, T. R., Maina, J., … Mouillot, D. (2016). Bright spots among the world's coral reefs. *Nature*, *535*(7612), 416–419.

Courcelle, J., & Hanawalt, P. C. (1999). RecQ and RecJ process blocked replication forks prior to the resumption of replication in UV-irradiated Escherichia coli. *Molecular & General Genetics : MGG*, *262*(3), 543–51. Retrieved from http://www.ncbi.nlm.nih.gov/pubmed/10589843

Courtial, L., Picco, V., Grover, R., Cormerais, Y., Rottier, C., Labbe, A., … Ferrier-Pagès, C.

(2017). The c-Jun N-terminal kinase prevents oxidative stress induced by UV and thermal stresses in corals and human cells. *Scientific Reports*, *7*(1), 45713.

Covington, A. K., & Whitfield, M. (1988). Recommendations for the determination of pH in sea water and estuarine waters. *Pure and Applied Chemistry*, *60*(6), 865–870.

Donner, S. D., Rickbeil, G. J. M., & Heron, S. F. (2017). A new, high-resolution global mass coral bleaching database. *PloS One*, *12*(4), e0175490.

EU Copernicus Marine Service. (2017). Global Ocean - In-Situ-Near-Real-Time Observations. Retrieved February 2, 2017, from http://marine.copernicus.eu

Goudet, J. (2005). HIERFSTAT, a package for R to compute and test hierarchical F-statistics. *Molecular Ecology Notes*, *5*(1), 184–186.

Hijmans, R. J. (2016). raster: Geographic Data Analysis and Modeling. Retrieved from https://cran.r-project.org/package=raster

Holderegger, R., Herrmann, D., Poncet, B., Gugerli, F., Thuiller, W., Taberlet, P., … Manel, S. (2008). Land ahead: using genome scans to identify molecular markers of adaptive relevance. *Plant Ecology & Diversity*, *1*(2), 273–283.

Howells, E. J., Berkelmans, R., van Oppen, M. J. H., Willis, B. L., & Bay, L. K. (2013). Historical thermal regimes define limits to coral acclimatization. *Ecology*, *94*(5), 1078–1088.

Hughes, T. P., Anderson, K. D., Connolly, S. R., Heron, S. F., Kerry, J. T., Lough, J. M., … Wilson, S. K. (2018). Spatial and temporal patterns of mass bleaching of corals in the Anthropocene. *Science*, *359*(6371), 80–83.

Hughes, T. P., Baird, A. H., Bellwood, D. R., Card, M., Connolly, S. R., Folke, C., … Roughgarden, J. (2003, August 15). Climate change, human impacts, and the resilience of coral reefs. *Science*.

Hughes, T. P., Kerry, J. T., Álvarez-Noriega, M., Álvarez-Romero, J. G., Anderson, K. D.,

Baird, A. H., … Wilson, S. K. (2017). Global warming and recurrent mass bleaching of corals. *Nature*, *543*(7645), 373–377.

Hughes, T. P., Kerry, J. T., Connolly, S. R., Baird, A. H., Eakin, C. M., Heron, S. F., … Torda, G. (2019, January 10). Ecological memory modifies the cumulative impact of recurrent climate extremes. *Nature Climate Change*. Nature Publishing Group.

Jensen, L. J., Julien, P., Kuhn, M., von Mering, C., Muller, J., Doerks, T., & Bork, P. (2008). eggNOG: automated construction and annotation of orthologous groups of genes. *Nucleic Acids Research*, *36*(Database issue), D250-4.

Jombart, T. (2008). adegenet: a R package for the multivariate analysis of genetic markers. *Bioinformatics*, *24*(11), 1403–1405.

Joost, S. (2006). *The geographical dimension of genetic diversity: a GIScience contribution for the conservation of animal genetic resources*. EPFL. Retrieved from https://infoscience.epfl.ch/record/64345?ln=en

Keller, L., & Waller, D. M. (2002). Inbreeding effects in wild populations. *Trends in Ecology & Evolution*, *17*(5), 230–241.

Kimura, T., Tun, K., & Chou, L. M. (2018). *Status of Coral Reefs in East Asian Seas Region: 2018*. Tokyo, Japan.

Krueck, N. C., Ahmadia, G. N., Green, A., Jones, G. P., Possingham, H. P., Riginos, C., … Mumby, P. J. (2017). Incorporating larval dispersal into MPA design for both conservation and fisheries. *Ecological Applications*, *27*(3), 925–941.

Krueger, T., Horwitz, N., Bodin, J., Giovani, M.-E., Escrig, S., Meibom, A., & Fine, M. (2017). Common reef-building coral in the Northern Red Sea resistant to elevated temperature and acidification. *Royal Society Open Science*, *4*(5), 170038.

Lee, K., Tong, L. T., Millero, F. J., Sabine, C. L., Dickson, A. G., Goyet, C., … Key, R. M. (2006). Global relationships of total alkalinity with salinity and temperature in surface

waters of the world's oceans. *Geophysical Research Letters*, *33*(19), L19605.

Leempoel, K., Duruz, S., Rochat, E., Widmer, I., Orozco-terWengel, P., & Joost, S. (2017). Simple Rules for an Efficient Use of Geographic Information Systems in Molecular Ecology. *Frontiers in Ecology and Evolution*, *5*, 33.

Lester, S., Halpern, B., Grorud-Colvert, K., Lubchenco, J., Ruttenberg, B., Gaines, S., … Warner, R. (2009). Biological effects within no-take marine reserves: a global synthesis. *Marine Ecology Progress Series*, *384*, 33–46.

Li, H., & Durbin, R. (2009). Fast and accurate short read alignment with Burrows-Wheeler transform. *Bioinformatics*, *25*(14), 1754–1760.

Li, H., Handsaker, B., Wysoker, A., Fennell, T., Ruan, J., Homer, N., … 1000 Genome Project Data Processing Subgroup, 1000 Genome Project Data Processing. (2009). The Sequence Alignment/Map format and SAMtools. *Bioinformatics (Oxford, England)*, *25*(16), 2078–9.

Liu, G., Strong, A. E., & Skirving, W. (2003). Remote sensing of sea surface temperatures during 2002 Barrier Reef coral bleaching. *Eos, Transactions American Geophysical Union*, *84*(15), 137–141.

Logan, C. A., Dunne, J. P., Eakin, C. M., & Donner, S. D. (2014). Incorporating adaptive responses into future projections of coral bleaching. *Global Change Biology*, *20*(1), 125–139.

Loukos, H., Vivier, F., Murphy, P. P., Harrison, D. E., & Le Quéré, C. (2000). Interannual variability of equatorial Pacific CO_2 fluxes estimated from temperature and salinity data. *Geophysical Research Letters*, *27*(12), 1735–1738.

Lukoschek, V., Riginos, C., & van Oppen, M. J. H. (2016). Congruent patterns of connectivity can inform management for broadcast spawning corals on the Great Barrier Reef. *Molecular Ecology*, *25*(13), 3065–3080.

657 Lundgren, P., Vera, J. C., Peplow, L., Manel, S., & van Oppen, M. J. H. (2013). Genotype -
658 environment correlations in corals from the Great Barrier Reef. *BMC Genetics*, *14*(1), 9.
659 Madden, T., & Coulouris, G. (2008). BLAST Command Line Applications User Manual
660 BLAST Command Line Applications User Manual - BLAST ® ... National Center for
661 Biotechnology Information (US). Retrieved from
662 http://www.ncbi.nlm.nih.gov/books/NBK279690/
663 Maina, J., McClanahan, T. R., Venus, V., Ateweberhan, M., & Madin, J. (2011). Global
664 gradients of coral exposure to environmental stresses and implications for local
665 management. *PLoS ONE*, *6*(8), e23064.
666 Maina, J., Venus, V., McClanahan, T. R., & Ateweberhan, M. (2008). Modelling
667 susceptibility of coral reefs to environmental stress using remote sensing data and GIS
668 models. *Ecological Modelling*, *212*(3), 180–199.
669 McKenna, A., Hanna, M., Banks, E., Sivachenko, A., Cibulskis, K., Kernytsky, A., …
670 DePristo, M. A. (2010). The Genome Analysis Toolkit: a MapReduce framework for
671 analyzing next-generation DNA sequencing data. *Genome Research*, *20*(9), 1297–303.
672 McKinney, W. (2010). Data Structures for Statistical Computing in Python. Retrieved from
673 http://conference.scipy.org/proceedings/scipy2010/mckinney.html
674 Moberg, F., & Folke, C. (1999). Ecological goods and services of coral reef ecosystems.
675 *Ecological Economics*, *29*(2), 215–233.
676 Mydlarz, L. D., McGinty, E. S., & Harvell, C. D. (2010). What are the physiological and
677 immunological responses of coral to climate warming and disease? *The Journal of*
678 *Experimental Biology*, *213*(6), 934–45.
679 Nakajima, Y., Nishikawa, A., Iguchi, A., & Sakai, K. (2010). Gene Flow and Genetic
680 Diversity of a Broadcast-Spawning Coral in Northern Peripheral Populations. *PLoS*
681 *ONE*, *5*(6), e11149.

NASA. (2016). NASA Earth Observations (NEO). Retrieved May 10, 2017, from http://neo.sci.gsfc.nasa.gov/

National Oceanic and Atmospheric Administration. (2017). NOAA DATA CATALOG. Retrieved February 2, 2017, from https://data.noaa.gov/dataset/

Neupane, A., Nepal, M. P., Benson, B. V, MacArthur, K. J., & Piya, S. (2013). Evolutionary history of mitogen-activated protein kinase (MAPK) genes in Lotus, Medicago, and Phaseolus. *Plant Signaling and Behavior*, *8*(11), e27189.

Nishikawa, A. (2008). Degree and Pattern of Gene Flow in Several Scleractinian Corals in the Ryukyu Archipelago, Southern Japan. *Https://Doi.Org/10.2984/1534-6188(2008)62[413:DAPOGF]2.0.CO;2*, *62*(3), 413–422.

Nosil, P., Funk, D. J., & Ortiz-Barrientos, D. (2009, February 1). Divergent selection and heterogeneous genomic divergence. *Molecular Ecology*. John Wiley & Sons, Ltd (10.1111).

OECD. (2017). *Marine protected areas : economics, management and effective policy mixes.* Paris: OECD Publishing.

Palumbi, S. R. (2003). Population genetics, demographic connectivity, and the design of marine reserves. *Ecological Applications*, *13*(1 SUPPL.), 146–158.

Palumbi, S. R., Barshis, D. J., Traylor-Knowles, N., & Bay, R. A. (2014). Mechanisms of reef coral resistance to future climate change. *Science*, *344*(6186). Retrieved from http://science.sciencemag.org/content/344/6186/895

Paris-Limouzy, C. B. (2011). Reef Interconnectivity/Larval Dispersal (pp. 881–889). Springer, Dordrecht.

Penin, L., Vidal-Dupiol, J., & Adjeroud, M. (2013). Response of coral assemblages to thermal stress: are bleaching intensity and spatial patterns consistent between events? *Environmental Monitoring and Assessment*, *185*(6), 5031–5042.

Pratchett, M. S., Thompson, C. A., Hoey, A. S., Cowman, P. F., & Wilson, S. K. (2018). Effects of Coral Bleaching and Coral Loss on the Structure and Function of Reef Fish Assemblages (pp. 265–293). Springer, Cham.

Python Software Foundation. (2018). Python Language Refrence, version 3.5. Retrieved from www.python.org

QGIS development team. (2009). QGIS Geographic Information System. Open Source Geospatial Foundation Project. Retrieved from http://www.qgis.org/

R Core Team. (2016). R: A Language and Environment for Statistical Computing. Retrieved from https://www.r-project.org/

Rellstab, C., Gugerli, F., Eckert, A. J., Hancock, A. M., & Holderegger, R. (2015). A practical guide to environmental association analysis in landscape genomics. *Molecular Ecology*, *24*(17), 4348–4370.

Riginos, C., Crandall, E. D., Liggins, L., Bongaerts, P., & Treml, E. A. (2016). Navigating the currents of seascape genomics: how spatial analyses can augment population genomic studies. *Current Zoology*, *62*, doi: 10.1093/cz/zow067.

Rochat, E., Leempoel, K., Vajana, E., Colli, L., Ajmone-Marsan, P., Joost, S. and the N. C. (2016). Map of genotype frequency change in autochtonous Moroccan sheep breeds due to global warming. In *Conference on Conservation genomics, May 3-6, 2016, Vairao, Portugal*.

Rodgers, K. S., Lorance, K., Richards Donà, A., Stender, Y., Lager, C., & Jokiel, P. L. (2017). Effectiveness of coral relocation as a mitigation strategy in Kāne'ohe Bay, Hawai'i. *PeerJ*, *5*, e3346.

Ryan, W. B. F., Carbotte, S. M., Coplan, J. O., O'Hara, S., Melkonian, A., Arko, R., … Zemsky, R. (2009). Global Multi-Resolution Topography synthesis. *Geochemistry, Geophysics, Geosystems*, *10*(3), n/a-n/a.

Sampayo, E. M., Franceschinis, L., Roff, G., Ridgway, T., Dove, S., & Hoegh-Guldberg, O. (2016). Coral symbioses under prolonged environmental change: living near tolerance range limits. *Scientific Reports*, *6*(1), 36271.

Seabold, S., & Perktold, J. (2010). Statsmodels: econometric and statistical modeling with Python. In *9th Python in Science Conference* (pp. 57–61). Retrieved from http://statsmodels.sourceforge.net/

Selig, E. R., & Bruno, J. F. (2010). A global analysis of the effectiveness of marine protected areas in preventing coral loss. *PloS One*, *5*(2), e9278.

Selmoni, O., Vajana, E., Guillaume, A., Rochat, E., & Joost, S. (2019). Sampling strategy optimization to increase statistical power in landscape genomics: a simulation-based approach. *Molecular Ecology Resources*, 1755–0998.13095.

Shanks, A. L., Grantham, B. A., & Carr, M. H. (2003). Propagule Dispersal Distance and the Size and Spacing of Marine Reserves. *Ecological Applications*, *13*(1).

Sharma, S., Doherty, K. M., Brosh, R. M., & Jr. (2006). Mechanisms of RecQ helicases in pathways of DNA metabolism and maintenance of genomic stability. *The Biochemical Journal*, *398*(3), 319–37.

Shinzato, C., Mungpakdee, S., Arakaki, N., & Satoh, N. (2015). Genome-wide SNP analysis explains coral diversity and recovery in the Ryukyu Archipelago. *Scientific Reports*, *5*(1), 18211.

Shinzato, C., Shoguchi, E., Kawashima, T., Hamada, M., Hisata, K., Tanaka, M., … Satoh, N. (2011). Using the Acropora digitifera genome to understand coral responses to environmental change. *Nature*, *476*(7360), 320–323.

Storey, J. D. (2003). The Positive False Discovery Rate: A Bayesian Interpretation and the q-Value. *Annals of Statistics*, *31*(6), 2013–2035.

Stubben, C., & Milligan, B. (2007). Estimating and Analyzing Demographic Models Using

the **popbio** Package in *R*. *Journal of Statistical Software*, *22*(11), 1–23.

Stucki, S., Orozco-terWengel, P., Bruford, M. W., Colli, L., Masembe, C., Negrini, R., … Consortium, the N. (2017). High performance computation of landscape genomic models integrating local indices of spatial association. *Molecular Ecology Resources*, *17*(5), 1072–1089.

Thomas, C. J., Lambrechts, J., Wolanski, E., Traag, V. A., Blondel, V. D., Deleersnijder, E., & Hanert, E. (2014). Numerical modelling and graph theory tools to study ecological connectivity in the Great Barrier Reef. *Ecological Modelling*, *272*, 160–174.

Thomas, L., Kennington, W. J., Evans, R. D., Kendrick, G. A., & Stat, M. (2017). Restricted gene flow and local adaptation highlight the vulnerability of high-latitude reefs to rapid environmental change. *Global Change Biology*, *23*(6), 2197–2205.

Thompson, D. M., & van Woesik, R. (2009). Corals escape bleaching in regions that recently and historically experienced frequent thermal stress. *Proceedings. Biological Sciences / The Royal Society*, *276*(1669), 2893–2901.

UNEP-WCMC, WorldFish-Center, WRI, & TNC. (2010). Global distribution of warm-water coral reefs, compiled from multiple sources including the Millennium Coral Reef Mapping Project. Version 1.3. Retrieved May 9, 2017, from http://data.unep-wcmc.org/datasets/1

Van der Auwera, G. A., Carneiro, M. O., Hartl, C., Poplin, R., del Angel, G., Levy-Moonshine, A., … DePristo, M. A. (2013). From FastQ Data to High-Confidence Variant Calls: The Genome Analysis Toolkit Best Practices Pipeline. In *Current Protocols in Bioinformatics* (Vol. 43, p. 11.10.1-11.10.33). Hoboken, NJ, USA: John Wiley & Sons, Inc.

van Etten, J. (2018). gdistance: Distances and Routes on Geographical Grids. Retrieved from https://cran.r-project.org/package=gdistance

van Oppen, M. J. H., Oliver, J. K., Putnam, H. M., & Gates, R. D. (2015a). Building coral reef resilience through assisted evolution. *Proceedings of the National Academy of Sciences of the United States of America*, *112*(8), 2307–13.

van Oppen, M. J. H., Oliver, J. K., Putnam, H. M., & Gates, R. D. (2015b). Building coral reef resilience through assisted evolution. *Proceedings of the National Academy of Sciences of the United States of America*, *112*(8), 2307–13.

Van Oppen, M. J. H., Willis, B. L., Van Rheede, T., & Miller, D. J. (2002). Spawning times, reproductive compatibilities and genetic structuring in the Acropora aspera group: evidence for natural hybridization and semi-permeable species boundaries in corals. *Molecular Ecology*, *11*(8), 1363–76.

Van Woesik, R., Irikawa, A., & Loya, Y. (2004). Coral Bleaching: Signs of Change in Southern Japan. In *Coral Health and Disease* (pp. 119–141). Berlin, Heidelberg: Springer Berlin Heidelberg.

Visel, A., Rubin, E. M., & Pennacchio, L. A. (2009). Genomic views of distant-acting enhancers. *Nature*, *461*(7261), 199–205.

Weir, B. S., & Cockerham, C. C. (1984). Estimating F-Statistics for the Analysis of Population Structure. *Evolution*, *38*(6), 1358.

Welle, P. D., Small, M. J., Doney, S. C., & Azevedo, I. L. (2017). Estimating the effect of multiple environmental stressors on coral bleaching and mortality. *PloS One*, *12*(5), e0175018.

Yamazato, K. (1999). Coral bleaching in Okinawa, 1980 vs 1998. *Journal of the Japanese Coral Reef Society*, *1999*(1), 83–87.

Young, C. N., Schopmeyer, S. A., & Lirman, D. (2012). A review of reef restoration and Coral propagation using the threatened genus Acropora in the Caribbean and western Atlantic. *Bulletin of Marine Science*, *88*(4), 1075–1098.

Zheng, X., Levine, D., Shen, J., Gogarten, S. M., Laurie, C., & Weir, B. S. (2012). A high-performance computing toolset for relatedness and principal component analysis of SNP data. *Bioinformatics*, *28*(24), 3326–3328.

Ziegler, M., Seneca, F. O., Yum, L. K., Palumbi, S. R., & Voolstra, C. R. (2017). Bacterial community dynamics are linked to patterns of coral heat tolerance. *Nature Communications*, *8*, 14213.

Figures

Figure 1. The study area. The Ryukyu Archipelago extends for more than 1,000 km in the north-western Pacific Ocean. The red circles display the 11 sites where samples were collected for the seascape genomics analysis (adapted from Shinzato, Mungpakdee, Arakaki, & Satoh, 2015).

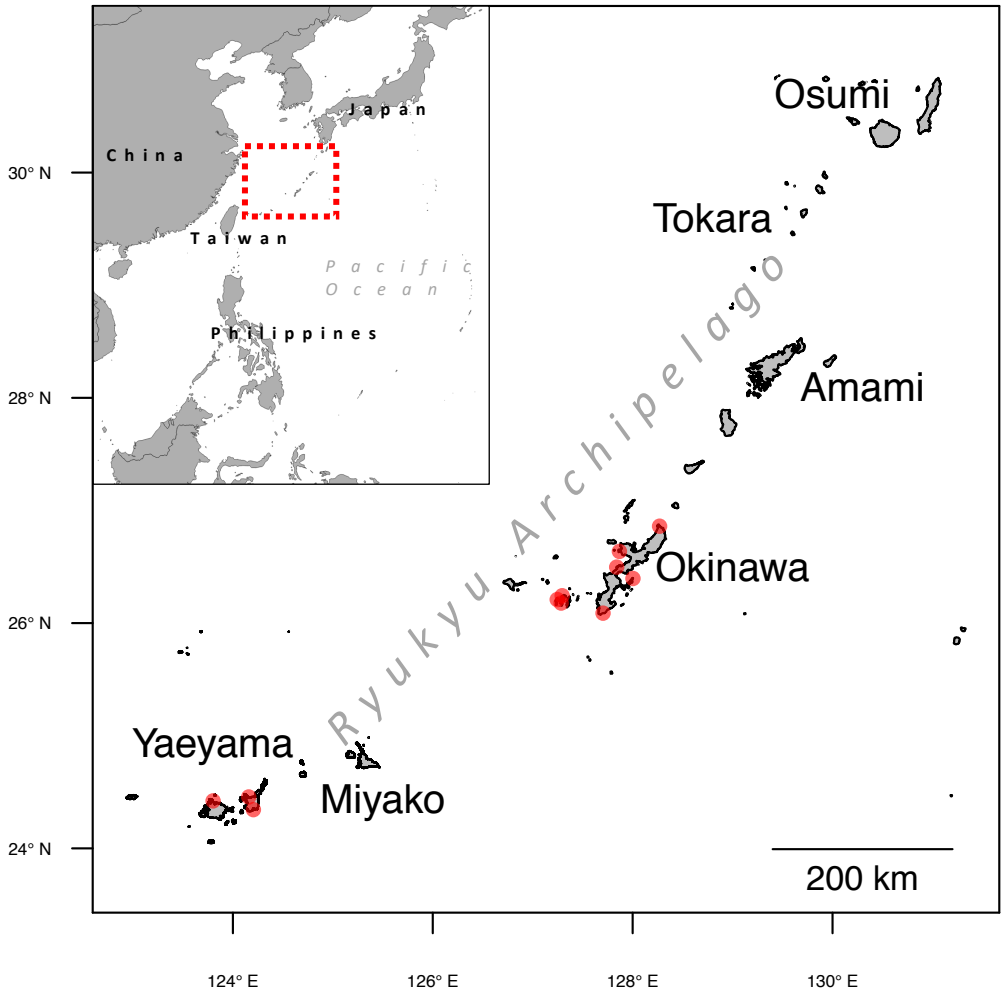

Figure 2. Workflow of the methods. The starting point for the analysis is the generation of genetic data describing the genotypes observed at different sampling locations (in this example, 4 sampling sites). In the seascape genomics analysis (A), these data are combined with environmental information to uncover genotypes whose frequencies are associated with specific climatic conditions (ENV). Such genotypes are defined as potentially adaptive. The model describing this link is then applied to environmental data at the scale of the whole reef system (B), to predict the probability of presence of the adaptive genotypes (green: high probability; red: low probability). The genetic data are also combined with sea current information to build a connectivity model (C) describing how sea distances correspond to genetic separation between sampling sites. This model is fitted with sea distance between all the reefs of the study area to predict (D) patterns of connectivity from (outbound) and to (inbound) each reef (green: high connectivity; red: low connectivity). Finally, predictions of the presence of adaptive genotypes and connectivity patterns are combined to assess the adaptive potential across the study area (E): reefs that are connected with sites that are likely to carry the adaptive genotype will have a higher adaptive potential (green), while those that are isolated will have lower adaptive potential (red).

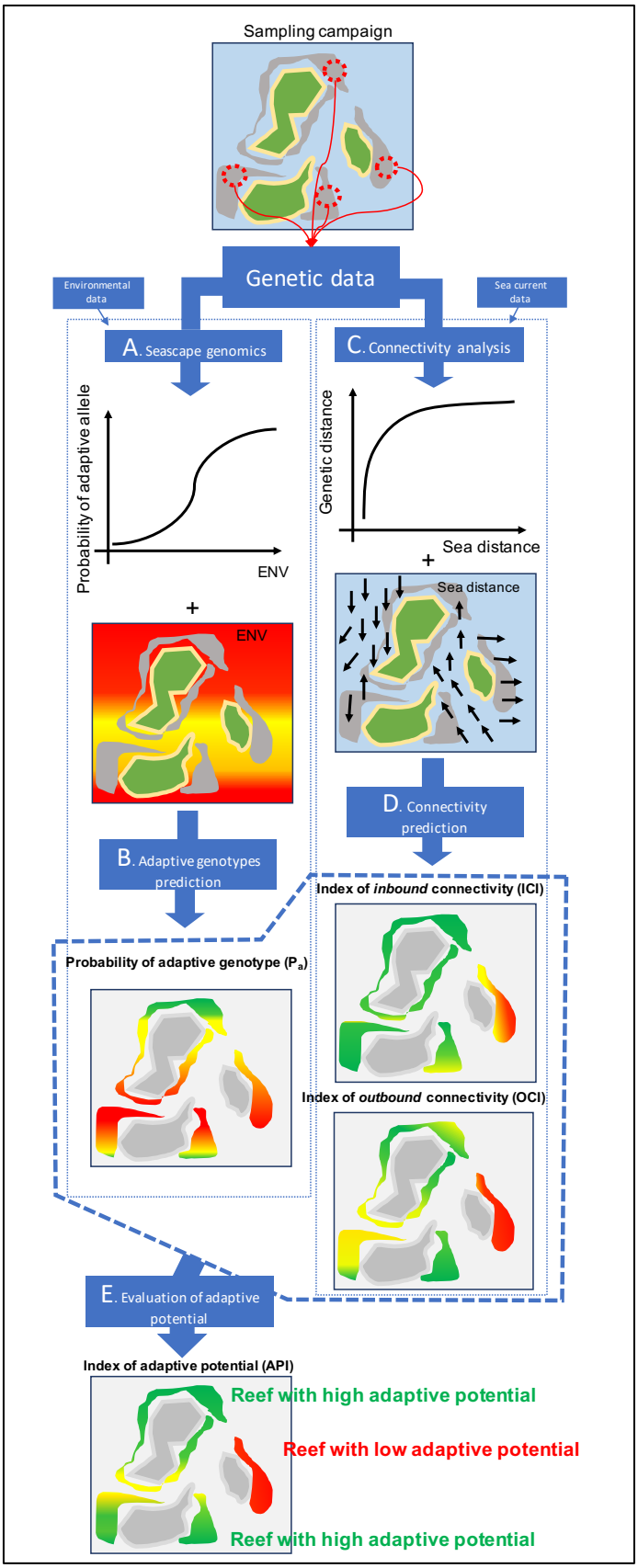
Sampling campaign
Genetic data
Environmental data
Sea current data
A. Seascape genomics
C. Connectivity analysis
Probability of adaptive allele
ENV
+
ENV
Genetic distance
Sea distance
+
Sea distance
B. Adaptive genotypes prediction
D. Connectivity prediction
Index of inbound connectivity (ICI)
Probability of adaptive genotype (Pa)
Index of outbound connectivity (OCI)
E. Evaluation of adaptive potential
Index of adaptive potential (API)
Reef with high adaptive potential
Reef with low adaptive potential
Reef with high adaptive potential

Figure 3. Cumulated probability of carrying adaptive genotypes vs DHW. The map shows the probability of presence of genotypes expected to be linked to adaptation to thermal stress across the study area and the neighbouring regions. Five gene-environment associations (SGEA2-6, Tab. 1) describing the association between distinct putative adaptive genotypes and DHW frequency were used to predict expected genotype frequencies. These expected frequencies were then averaged to compute the cumulated probability of adaptive genotypes. The dashed box highlights the position of the Ryukyu Archipelago.

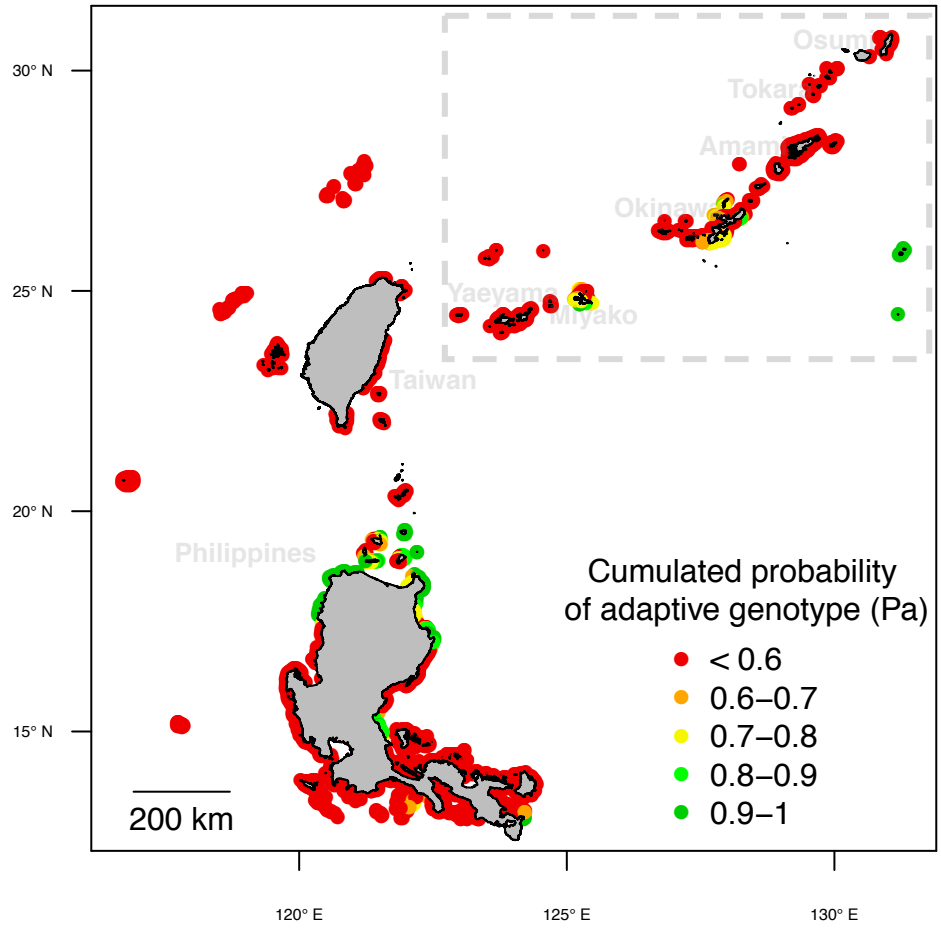

Figure 4. Connectivity indices. The maps show the potential connectivity to (a) and from (b) every reef of the Ryukyu Archipelago. In (a), the inbound connectivity index (ICI) represents the total area (in km^2) of the reefs that are connected to the focal reef with a pFst<0.02 (pFst toward the focal reef). In (b), the outbound connectivity index (OCI) displays the total area of the reefs that are connected from the focal reef with a pFst<0.02 (pFst from the focal reef).

a) Inbound connectivity

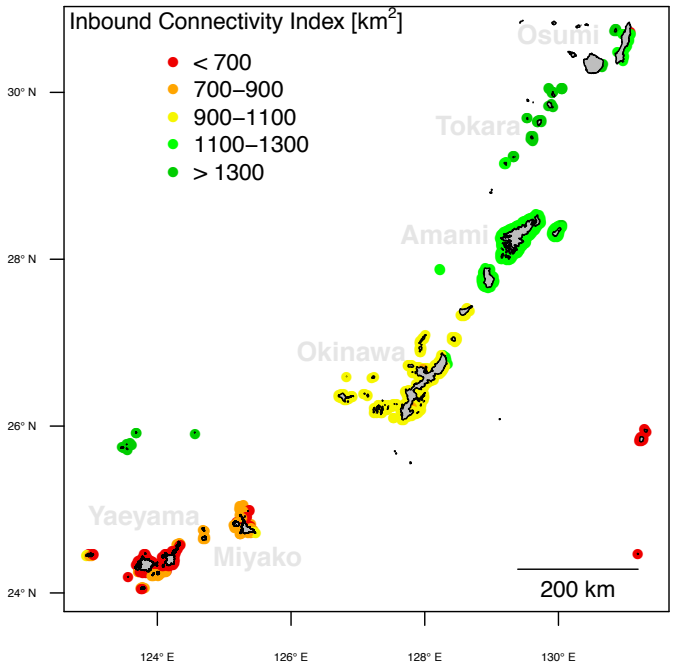

b) Outbound connectivity

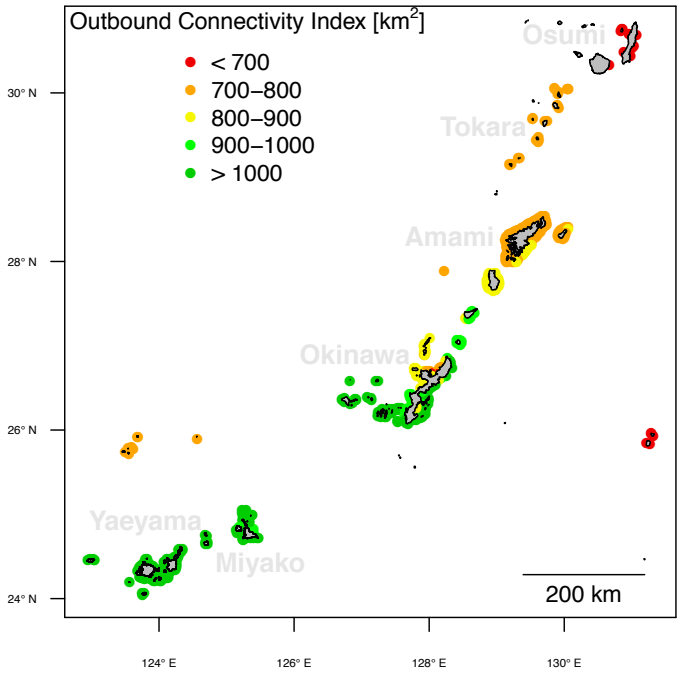
Outbound Connectivity Index [km2]
< 700
700–800
800–900
900–1000
> 1000
Osumi
Tokara
Amami
Okinawa
Yaeyama
Miyako
200 km
30° N
28° N
26° N
24° N
124° E
126° E
128° E
130° E

Figure 5. Index of adaptive potential. The map displays the index of adaptive potential (API) against thermal stress (DHW frequency) for every reef of the study area. This index represents the sum of weighted areas of reefs connected to the focal reef with a pFst<0.02 (pFst toward the focal reef). The weight applied correspond to the probability of presence of adaptive genotypes (Pa).

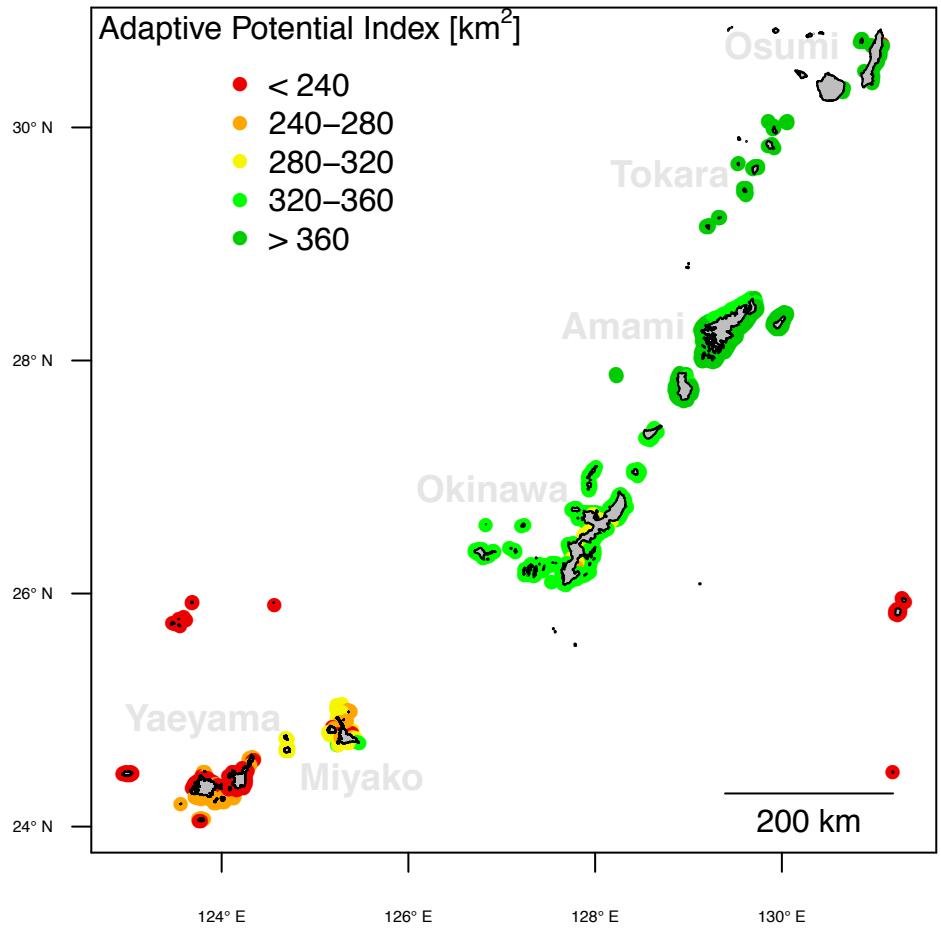

Box 1. Examples of applications of ICI (a) and API (b) in conservation management

a) Marine protected areas (MPAs)

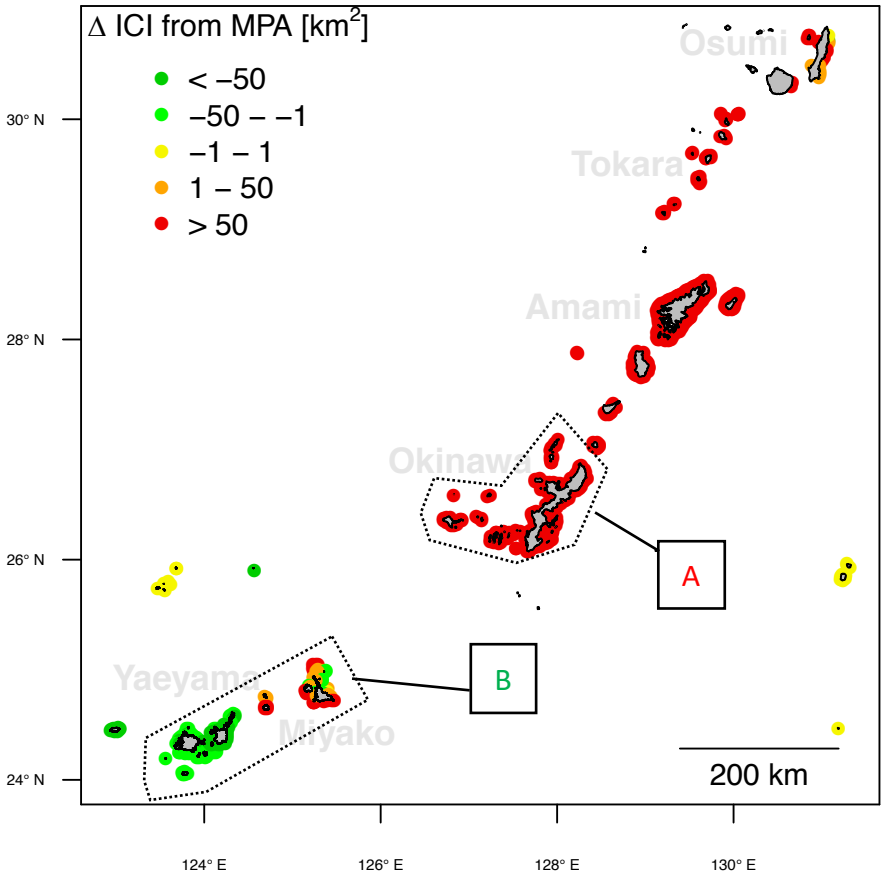

Two different locations for MPA of the same size are compared. In the first location (A), the MPA is established in Okinawa, and in Miyako and Yaeyama for the second one (B). For every reef of the Ryukyu Archipelago, we computed the ICI from each of the two MPA locations. In this map, we show the difference of the two ICI ($\Delta ICI = ICI_A - ICI_B$). An overall $\overline{\Delta ICI} = +40\ km^2$ indicates that the MPA in (A) is expected to produce a stronger increase of the inbound connectivity of reefs of the study area. However, these positive effects do not extend to southern reefs (Yaeyama and Miyako), where an MPA in (B) would provide a stronger increase in ICI.

b) Coral nurseries (CNs)

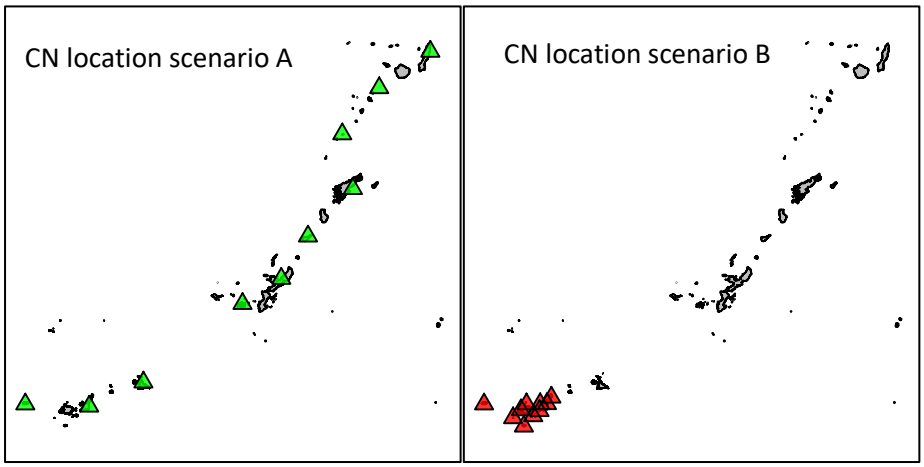

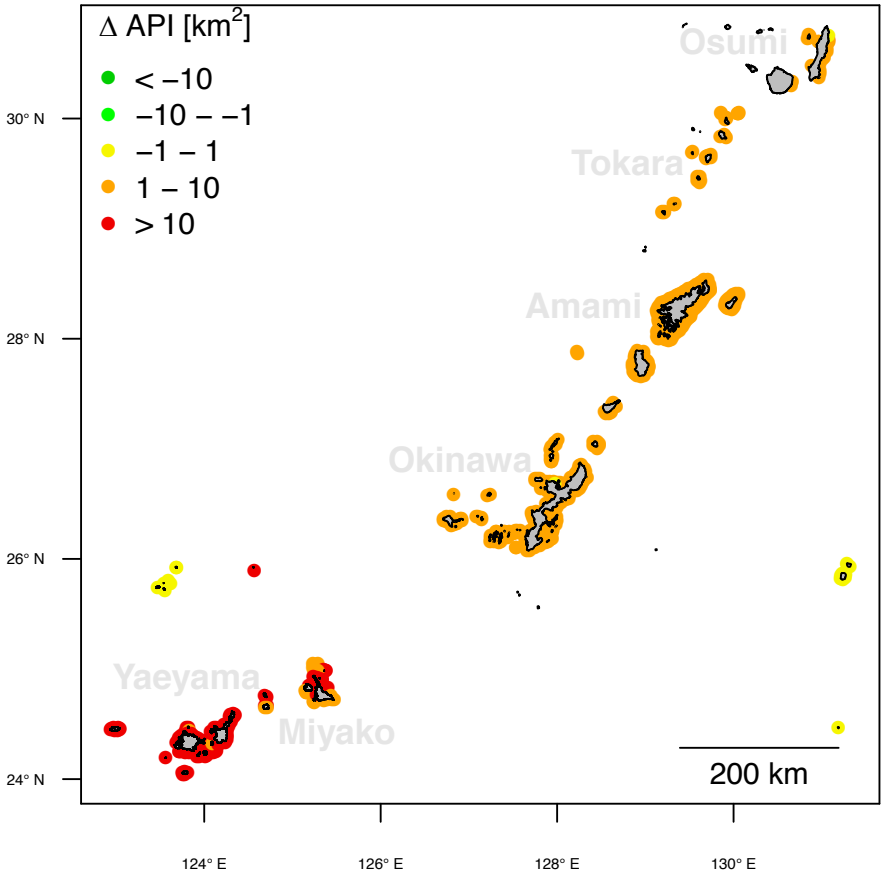

The different locations of two CNs network are compared. Each network is composed of 10 reefs where the P_a was set equal to 1 (simulating the restoration via transplantation of adapted colonies). In the first scenario (A, green triangles), CNs are established in the island of Yaeyama. In the second scenario (B, red triangles), CNs are located all across the archipelago. For every reef of the study area, API is calculated under the two network scenarios (A and B). The map shows the difference of API between the two locations ($\Delta API = API_A - API_B$). Overall $\overline{\Delta API}$ is $+5\ km^2$, therefore suggesting that the CN network A provides a general increase of adaptive potential in the study area. Such positive effects are visible in any region of the Archipelago.

1 **Tables**

Table 1. Significant genotype-environment associations. The seascape genomics analysis using the SamBada method detected 6 significant (qG and qW<0.001) genotype-environment associations (SGEA). This table shows, for each SGEA, the genomic position of the concerned SNP (in the format scaffoldID:position; Position), the q-values related to the G-score (qG) and the Wald-score (qW) of the association model, the concerned environmental variables (Env. Var.), the number of predicted genes in a ± 250 kb window around the concerned SNP (with the number of predicted genes annotated by similarity with a known gene, in brackets) and the related annotations on the eukaryote cluster of orthologous genes (KOG; with the frequency of the annotation across the reference genome, in brackets).

ID	Position	q_G	q_W	Env. Var	Genes	Annotated KOG
SGEA1	NW_015441190.1:582812	1.5E-08	1.3E-04	SST variance in April	18 (6)	KOG4088: Signal sequence receptor delta (0.001); KOG0351: DNA helicase (0.041); KOG4585: transposon protein (0.053)
SGEA2	NW_015441080.1:208400	1.1E-09	5.5E-05	DHW frequency	21 (18)	KOG0120: splicing factor U2AF (0.001); KOG4193: G- protein-coupled receptor (0.059); KOG0777: geranylgeranyl diphosphate synthase (0.001); KOG0157: Cytochrome p450 (0.011); KOG3656: receptor (0.324); KOG2358: NFU1 iron-sulfur cluster scaffold homolog (0.002)
SGEA3	NW_015441121.1:665651	1.7E-07	1.5E-04	DHW frequency	14 (2)	KOG0192: protein kinase kinase kinase (0.036); KOG0619: leucine rich repeat (0.061); KOG3744: jnk1 mapk8-associated membrane protein (0.001)
SGEA4	NW_015441282.1:27616	5.8E-06	6.9E-04	DHW frequency	11 (2)	KOG0351: DNA helicase (0.041); KOG4373: Exonuclease 3'-5' domain containing 2 (0.013)
SGEA5	NW_015441785.1:16151	6.6E-06	9.5E-04	DHW frequency	5 (2)	KOG0351: DNA helicase (0.041); KOG4373: Exonuclease 3'-5' domain containing 2 (0.013)
SGEA6	NW_015442197.1:32233	4.14E-06	9.5E-04	DHW frequency	1 (1)	KOG0351: DNA helicase (0.041); KOG4373: Exonuclease 3'-5' domain containing 2 (0.013)

2

Table 2. Field report of the 2016 mass bleaching event. The table shows the severity and mortality associated with the 2016 bleaching event as reported by Global Coral Reef Monitoring Network (Kimura et al., 2018). For every region surveyed in this report (identified by an ID and a region name), we show the corresponding region in our study and the associated average API, P_a and degree of heat stress in 2016 (estimated as the number of days with DHW>4°C). Colours scales highlight the value variations of each column.

ID	Region Name	Region Area (this study)	Bleaching [%]	Morality [%]	API [km2]	Pa	Heat Stress [# of days]
3	Amami Islands	Amami	8.5	2.1	371	0.26	68
4	Okinawa Island, East coast	Okinawa	21	0.7	339	0.60	69
5	Okinawa Island, West coast	Okinawa	13.1	4.3	328	0.36	75
6	Okinawa Outer Islands	Okinawa	48.4	13.5	336	0.70	82
7	Kerama Islands	Okinawa	7.3	5.4	334	0.08	81
9	Miyako Island	Miyako	68.8	31	282	0.61	84
10	Miyako Outer Reefs	Miyako	70.1	67.5	293	0.69	85
11	Ishigaki Island, East coast	Yaeyama	47.9	8.8	230	0.38	81
12	Ishigaki Island, West coast	Yaeyama	63.2	14.8	226	0.11	80
13	Sekisei Lagoon, North	Yaeyama	91.5	46.9	225	0.16	81
14	Sekisei Lagoon, East	Yaeyama	99.5	67.9	238	0.29	82
15	Sekisei Lagoon, Center	Yaeyama	94.9	49.7	241	0.24	82
16	Sekisei Lagoon, South	Yaeyama	98.2	50	254	0.19	83
17	Iriomote Islands	Yaeyama	94.3	34.8	236	0.28	80